Transportation Research Part D 118 (2023) 103724

Contents lists available at ScienceDirect

Transportation Research Part D

journal homepage: www.elsevier.com/locate/trd

Cost-effective electric bus resource assignment based on optimized charging and decision robustness

Qiuzi Chen [a], Chenming Niu [a], Ran Tu [a,*], Tiezhu Li [a], An Wang [b], Dengbo He [c]

[a] School of Transportation, Southeast University, Nanjing, China
[b] Massachusetts Institute of Technology, Cambridge, United States
[c] Systems Hub, Department of Civil and Environmental Engineering, The Hong Kong University of Science and Technology, Guangzhou, China

ARTICLE INFO

Keywords:
Battery electric bus
Charging strategy
Charging station capacity
Fleet composition
Energy consumption uncertainty

ABSTRACT

This paper explores a cost-efficient resource assignment for urban battery-electric-buses (BEBs) considering decision robustness based on the optimized charging plan. A network flow model was proposed to minimize the operation cost with mixed fleet, nonlinear charging and the constraint of charging station capacity. A sensitivity analysis was implemented using samples generated from clustered real-world data to simulate traffic-dependent bus travel time and energy consumption. The result shows that charging at night or with short duration in the daytime significantly increases the operation cost. Sufficient charging resources improve the robustness of the charging plan, while economic benefits merely increase when the charging station capacity reaches a certain threshold. Bus operators can reduce the investment in chargers to ensure both economic benefits and operation stability. When bus routes are longer with higher energy consumption, buses with medium or high battery capacity become more demanding, while the requirement on charging resources remains stable.

1. Introduction

Bus electrification is one of the main strategies to tackle climate and energy issues on the urban scale. In 2020, the proportion of alternative fuel buses in China is 66.2%, and it is proposed to reach 72% in 2025 (The State Council of People's Republic of China, 2021). Compared with traditional diesel-powered buses, battery-electric buses (BEB) have been proven to be more ecologically beneficial and cost-competitive from the life cycle perspective (Dunn et al., 2015; Wu et al., 2018; Quarles et al., 2020). Despite the development of the technology, difficulties still exist in the application and operation of BEBs.

The main challenge in the operation stage is the charging planning problem. Compared with diesel-powered bus operation, BEB operation needs to plan additional charging schedules besides service trips. Among charging strategies for plug-in BEBs, opportunity charging at terminal stops and depot charging at nighttime are most widely used due to the simplicity of execution (Jefferies and Göhlich, 2020). However, a more flexible and optimized charging strategy can significantly improve operation efficiency, leading to a substantial cost reduction (Lajunen and Lipman, 2016).

Due to the mileage limitation of BEBs, the urban bus operation is sensitive to existing resources, including bus fleets and charging facilities. On the one hand, the fixed number of chargers restricts the charging opportunities of vehicles, leading to the need for a larger bus fleet size or buses with a higher battery capacity. On the other hand, higher battery capacity leads to higher purchase costs, while buses with lower battery capacity will need more frequent recharging. The composition of the fleet and the number

* Corresponding author.
E-mail addresses: qiuzi.chen@outlook.com (Q. Chen), ncm13949349506@163.com (C. Niu), turancoolgal@seu.edu.cn (R. Tu), litiezhu@seu.edu.cn (T. Li), an_wang@mit.edu (A. Wang), dengbohe@ust.hk (D. He).

https://doi.org/10.1016/j.trd.2023.103724
Received 14 September 2022; Received in revised form 8 March 2023; Accepted 26 March 2023
Available online 31 March 2023

of charging facilities jointly affect the charging schedule, and restrict each other at the same time. Therefore, it is also desired for operators to decide the best assignment of existing resources in the charging plan.

Regarding the fleet, vehicles with different sizes have varied driving ranges, energy consumption and prices, leading to the fleet composition problem (Yıldırım and Yıldız, 2021). Meanwhile, the trip travel time and energy consumption of BEB are affected by several factors, such as traffic conditions, passenger demands, and driving behaviors (Bie et al., 2021). This uncertainty raises concerns about decision robustness, especially for BEB systems with higher fragility than traditional diesel buses.

This study aims to evaluate the cost-effectiveness and robustness of resource assignment in BEB operation, including charger assignment and fleet composition, based on the optimal charging schedule. A BEB charging scheduling optimization problem is proposed with multiple vehicle types, battery nonlinear charging, and charging station capacity constraints. Variations of trip travel time and energy consumption are considered by integrating the optimization model with trip samples generated from real-world distribution. A real-world case study demonstrates the effectiveness of the proposed method and the relationship among the cost of charging strategies, fleet composition, and charging resources. Based on the sensitivity analysis, the impact of trip distance and energy consumption level is further discussed.

2. Literature review

The basic task of BEB charging planning optimization is the charging scheduling problem, which aims to minimize the operating and electricity cost by arranging charging events according to charging demand and existing charging resources (Perumal et al., 2021). Some research on charging scheduling takes the bus schedule as a predetermined input, and optimize the place and time point to recharge BEBs (Gao et al., 2018; He et al., 2020; Liu et al., 2021). In practice, however, the charging schedule is closely related to the trip-wide energy consumption and travel time; therefore, the bus schedule should also be considered in the optimization. Adler (2014) integrated traditional vehicle scheduling problem (VSP), which assigns buses to serve a given set of trips (Bunte and Kliewer, 2009), with the refueling scheduling process, and proposed a widely adopted network flow model with Alternative-Fuel Vehicle Scheduling Problem (AFVSP). Wen et al. (2016) extended AFVSP to electric vehicle scheduling problem (EVSP), and presented an adaptive large neighborhood search (ALNS) algorithm to solve it.

One of the major features of electric vehicles compared with diesel-powered vehicles is the nonlinear charging characteristics. The battery in an electric vehicle is usually charged with a constant current–constant voltage (CC-CV) scheme (Pelletier et al., 2017). To simulate the practical charging process, the piecewise linear approximation was adopted in current studies to model a CC-CV charging curve (Montoya et al., 2017; Zhang et al., 2021b; Zhou et al., 2022a). To tackle the problem of the increased computation complexity from the nonlinear charging, Zhang et al. (2021a) proposed an ALNS algorithm for EVSP considering nonlinear charging, which can provide high-quality solutions much faster than the exact approach for a large-scale network.

To investigate systematic optimization, operators should also consider the use of resources in charging planning, including bus fleets and charging facilities. By combining charging scheduling with fleet composition, existing studies reduced the operation cost with a mixed bus fleet with multiple bus types (Olsen et al., 2020; Rinaldi et al., 2020; Yao et al., 2020). Considering the vehicle as the demand-side in the BEB charging network, the charging facilities are regarded as suppliers with limited service capabilities. To fully utilize charging resources, a few studies proposed a systematic optimization for bus schedules, fleet composition, and charger deployment for a years-long investment problem (Rogge et al., 2018; Wang et al., 2022; He et al., 2022). Regarding the short-term charging resource assignment, evaluations can be conducted considering the charging station constraints, and the problem can be formulated by using time-expanded nodes (Li, 2014; Tang et al., 2019; Wu et al., 2022) or discrete time slots (Zhang et al., 2021b; Liu et al., 2021) in the network flow model.

Despite the increasing number of studies on BEB optimization, most assume trip energy consumption as a static parameter, ignoring the impact of uncertain energy consumption due to uncertain traffic conditions. Some studies considered the uncertainty by integrating an energy consumption distribution (Bie et al., 2021; Lee et al., 2021) or a robust optimization (Jiang and Zhang, 2021; Zhou et al., 2022b), while the influence of the traffic-dependent energy consumption on the decision of the resource assignment is under investigation. In addition, the sensitivity of such decisions on the route length and energy consumption is unclear.

To summarize, BEB charging planning problem mainly includes two tasks: charging scheduling and resources assignment, which are affected by vehicle scheduling, fleet composition, charging station capacity, battery nonlinear charging and energy consumption uncertainty. As shown in Table 1, few state-of-the-art studies on BEB charging planning have considered all the influencing factors. To fill this gap, this study develops a methodology to find the most cost-effective and robust resource assignment that can adapt to most circumstances according to the optimal charging schedule. The contributions of this study can be presented as follows.

- An optimization model for charging planning is established to minimize daily operating costs considering vehicle scheduling, multiple vehicle types, battery nonlinear charging, and charging station capacity. An ALNS algorithm is developed to solve large-scale problems.
- Trip energy consumption uncertainty is considered by integrating the optimization model with trip samples generated from real-world distribution. The operational cost-effectiveness of the BEB resource assignment is evaluated considering decision robustness.
- A real-world case study and the sensitivity analysis regarding the length of the route is conducted. General and robust decisions are concluded for the bus fleet composition and the station-wide charging capacity.

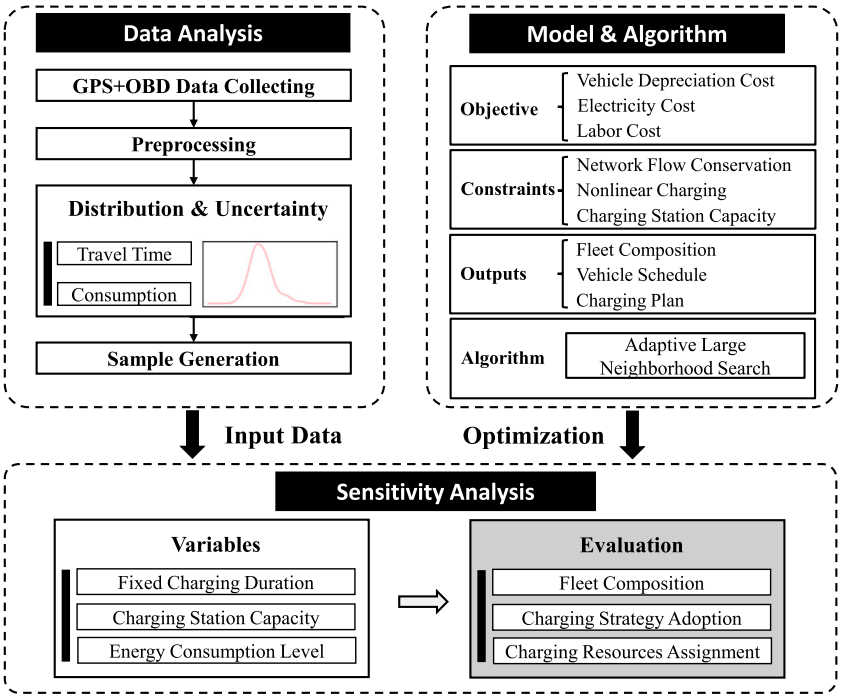

Fig. 1. Flow chart of this study.

Table 1
Overview of the literature on BEB charging planning.

Authors	Vehicle scheduling	Multiple vehicle type	Charging station capacity	Nonlinear charging	Energy consumption uncertainty	Algorithm
Li (2014)	✓		✓			B&P Truncated CG
Wen et al. (2016)	✓					ALNS
Rogge et al. (2018)	✓	✓	✓			GA
Gao et al. (2018)			✓			GA
Tang et al. (2019)	✓		✓			B&P
Zhang et al. (2021b)	✓		✓	✓		B&P
Zhang et al. (2021a)	✓	✓		✓		ALNS
Yıldırım and Yıldız (2021)	✓	✓				CG
Liu et al. (2021)			✓			CG
Jiang and Zhang (2021)	✓				✓	B&P
Bie et al. (2021)	✓				✓	NSGA-ii
Zhou et al. (2022b)	✓	✓			✓	CPLEX
Zhou et al. (2022a)	✓			✓		CPLEX
Wu et al. (2022)	✓		✓			Tailored B&P
Wang et al. (2022)	✓	✓	✓			Gurobi
He et al. (2022)	✓	✓	✓			CPLEX
This paper	✓	✓	✓	✓	✓	ALNS

3. Methodology

The methodology of this study is outlined in Fig. 1. First, the bus operation is surveyed, and the driving records are analyzed. The trip travel time and energy consumption samples are generated using the distribution derived from real-world data. Second, an electric vehicle scheduling problem with charging station capacity and nonlinear charging (EVSP-CSC-NL) is formulated, and an ALNS algorithm is proposed to solve the optimization. Finally, the charging plan with resource assignment recommendations is decided from the optimization, with the consideration of the traffic-dependent randomness in trip travel time and energy consumption. Appendix A summarizes the definitions of variables and parameters discussed in this section.

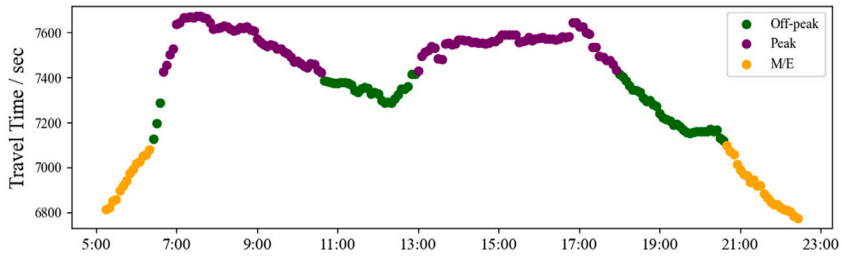

Fig. 2. Trip clustering according to historical average travel time *(M/E refers to the morning/evening period)*.

3.1. Data description and preprocessing

The global positioning system (GPS) and on-board diagnostics (OBD) system were used to collect the second-by-second operation data of five BEBs from bus Line 4 in Nanjing from April 22, 2021, to April 27, 2021. In total, 1,305,087 pieces of data, including second-by-second position, speed, battery voltage, and current, were collected. Daily service of Line 4 starts at 05:30 AM and ends at 11:30 PM with 64 round trips in timetable per day, 24.8 km per round trip. Each round trip includes a dispatched trip from the terminal and a return trip to the terminal. All vehicles are charged at the same station.

The data are first preprocessed with the following steps:

1. Delete the data outside the operation area according to GPS coordinates.
2. Delete the data with invalid values.
3. Delete outlier data according to vehicle acceleration referring to Farzaneh et al. (2014).
   - An upper limit of the 99-percentile value for instantaneous acceleration.
   - A lower limit of -4.4704 m/s^2 for instantaneous deceleration.
4. For missing data, if the time interval between two consecutive records is less than 10 s, use linear interpolation to fill the gap.

After preprocessing, the data are divided into 108 round trips. For each trip, average speed and energy consumption were extracted. The total energy consumption over time T is illustrated in Eq. (1), where U_t and I_t are the instantaneous output voltage and current of the battery.

$$E_{cons} = \int_0^T U(t)I(t)\mathrm{d}t = \frac{1}{1000 \times 3600} \cdot \sum_{t=1}^{T} U_t I_t \tag{1}$$

3.2. Trips clustering and sample generation

To explore the influence of trip energy and travel time variation on the decision robustness, we generate 100 samples, each containing a full-day bus service schedule, based on the real-world operation data to simulate traffic-dependent travel time and energy consumption of each trip. To distinguish trips from different periods of a day, the K-Means method was used to cluster all the trip records into three groups, namely peak, off-peak, and morning/evening trips (Fig. 2), according to the historical average travel time of Line 4 captured by the AMAP API (AMAP). For each scheduled trip, one pair of travel time and energy consumption belonging to the same trip from the corresponding group is randomly selected. Fig. 3 illustrates the process of sample generation. As a result, each sample is composed of all the service trips of the studied bus lines in one day, and each trip includes a randomly selected pair of travel time and energy consumption from the clustered real-world dataset.

3.3. Modeling approach

3.3.1. Problem description

In this study, we consider a single-depot bus network with one charging station and multiple types of BEBs. At the beginning of the operation, vehicles are dispatched from the depot to terminals for the day's service. After finishing all tasks, they return to the depot to park and get charged. During the operation, vehicles are allowed to dwell or park at terminals between service tasks and get recharged at the charging station, which is integrated into the terminal. The EVSP-CSC-NL proposed in this study aims to find the optimal vehicle schedule, charging plan and fleet composition of the network, considering the nonlinear charging characteristics of BEBs, and charging station capacity constraints with the following assumptions.

- Vehicles will be fully charged at the depot after finishing all tasks for the day to ensure that vehicles have enough power for the next day's operation. Charging resources at the depot are assumed sufficient.

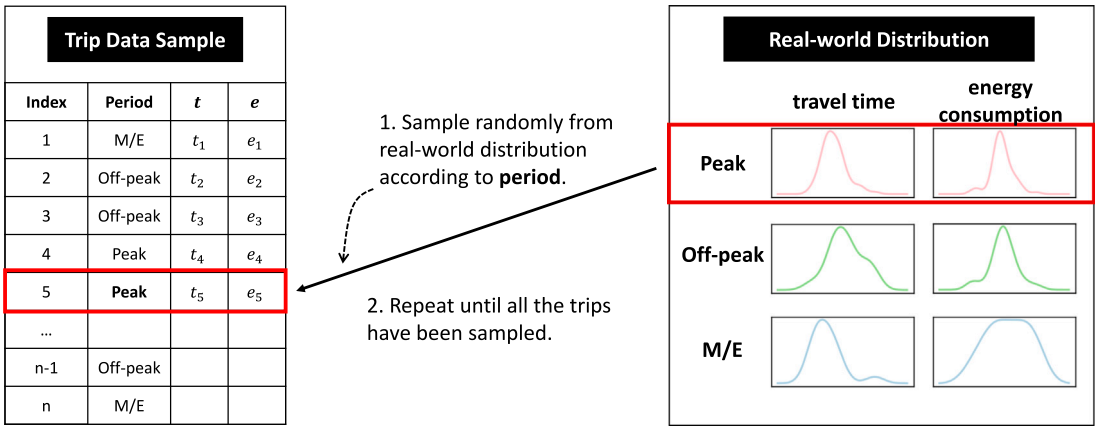

Fig. 3. Illustration of the sample generation method *(M/E refers to the morning/evening period)*.

- Vehicles are charged at the same charging station during operation, which is reasonable because we only consider the single depot operation mode.
- For the convenience of management, vehicles are only allowed to be charged for a fixed duration at most each time during daytime operation. If a vehicle is fully charged within the fixed duration, then it should dwell in the parking lot before next service task.

3.3.2. Network flow model

The model is defined on a directed multigraph $G = (N, A)$ where N and A represent all nodes and arcs in the graph. For bus type decision, we first defined bus type set $K = \{1, 2, \ldots\}$, in which each bus type $k \in K$ corresponds to battery capacity E^k. $N = D \cup T \cup F$ represents all nodes in the graph. D represents all depot nodes. For single depot operation mode, $D = \{o, d\}$ includes start and end nodes. For a trip node $i \in T$, the start time, travel time, and trip energy consumption are defined as s_i, t_i and e_i^k respectively, and corresponds to a recharging node $f_i \in F$.

In a network flow model, an arc $(i, j) \in A$ represents the connection, the deadhead trip between nodes i and j. There are four types of arcs in this paper:

- Deadhead trips from the depot, where $i \in \{o\}$, $j \in T$.
- Deadhead trips returning to the depot, where $i \in T$, $j \in \{d\}$.
- Deadhead trips between service trips, where $i, j \in T$ and $i \neq j$.
- Deadhead trips between service trips and recharging events, where $i \in T$ and $j \in F$, or $i \in F$ and $j \in T$. Due to the correspondence between service trips and recharging events, arc (i, f_i) is linked only if $i \in T$.

For arc $(i, j) \in A$, travel time t_{ij} and energy consumption e_{ij}^k are defined. For simplification, we use the notation $\delta^-(i)$ and $\delta^+(i)$ to represent arcs that end and start at node i.

Time-expanded nodes are used to count the number of recharging vehicles, which have also been adopted in previous studies such as Li (2014) and Tang et al. (2019). We assume that each recharging event takes $\beta \cdot U$ minutes, where β represents a fixed time interval, and U represents the number of unit intervals in one recharging event. Let $R = \{r_1, r_2, \ldots\}$ denotes set of recharging time divisions. Each time division $r \in R$ corresponds to a start time s_r. For $r \in R$, let $b^u(r)$ denotes the time division u intervals ahead of r. The number of BEBs being charged at the charging station can be calculated as the total number of vehicles selecting the time division r, $b^1(r) \ldots b^{U-1}(r)$. Let I denotes set of time division indicators. Indicators $(f, r) \in I$ represent the connection between recharging node $f \in F$ and time division $r \in R$.

A sample directed graph is presented in Fig. 4. The graph contains four service trips from 6:20 to 9:20. When time interval $\beta = 10$ min and fixed charging duration $\beta \cdot U = 30$ min, operation duration from 8:00 to 9:00 is divided into four recharging time divisions of 30 min each. Assuming the travel time of all deadhead trips is five minutes, a feasible schedule including trip chains of two BEBs (regardless of vehicle type) is shown in the graph. The first BEB executes trip t_1 and t_3 continuously without recharging because the interval between t_1 and t_3 was less than 30 min. The second BEB gets recharged at the charging station from 8:00 to 8:30 after performing service trip t_2 and continues with trip t_4 after f_2. Note that infeasible arcs should be deleted before running the optimization algorithm to fasten the computation.

The binary variable x_{ij}^k represents the connections of deadhead trips in the graph, where $(i, j) \in A$ is the arc of two nodes. The binary variable x_{fr}^k represents the decision of recharging time, where $(f, r) \in I$ is the time division indicators.

Let y_i^k denotes the remaining battery storage (kWh) of a bus of type k at the beginning of node $i \in N$. For recharging event $f \in F$, let s_f denotes the start time of f, and $\overline{y_f^k}$ denotes the remaining battery storage (kWh) of a bus of type k when f is finished.

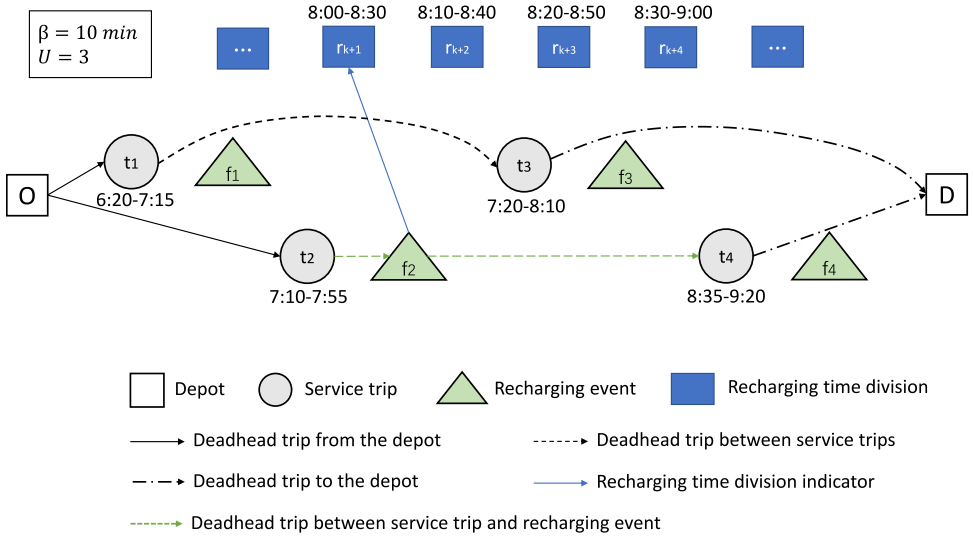

Fig. 4. Illustration of the directed graph.

To model the nonlinear charging process of the lithium-ion battery, a piecewise linear formulation proposed in Zhang et al. (2021a) is adopted. Let $B^k = \{0, 1, \dots, m^k\}$ denote the set of breakpoints of the charging function for vehicle type $k \in K$, where m^k is the number of the breakpoints. Let (t_b^k, y_b^k) represent the charging time and battery storage (kWh) corresponding to each breakpoint. Continuous variables τ_f^k and $\overline{\tau_f^k}$ represent the corresponding start and end time (in the charging function) of recharging event $f \in F$, respectively. Let binary variables w_{fb}^k and $\overline{w_{fb}^k}$ equal 1, $b \in B^k \setminus \{0\}$, if the start and end battery storage of recharging event $f \in F$ is between y_{b-1}^k and y_b^k. Continuous variables $\lambda_{fb}^k, \overline{\lambda_{fb}^k} \in [0, 1]$ are the coefficients associated with the breakpoint in the piecewise linear charging function at the beginning and end of the recharging event, respectively.

The mathematical model is formulated as follows:

$$\min \quad z_1 + z_2 + z_3 \tag{2}$$

$$z_1 = \sum_{k \in K} \sum_{(i,j) \in \delta^+(o)} c^k x_{ij}^k \tag{3}$$

$$z_2 = \sum_{r \in R} \sum_{k \in K} \sum_{f \in F} (\overline{y_f^k} - y_f^k) c_e x_{fr}^k + \sum_{k \in K} \sum_{i \in T} [E^k - (y_i^k - e_i^k - e_{id}^k)] c_e x_{id}^k \tag{4}$$

$$z_3 = \sum_{k \in K} \sum_{(i,j) \in A} (t_i + t_{ij}) c_t x_{ij}^k \tag{5}$$

Subject to:

$$\sum_{k \in K} \sum_{(i,j) \in \delta^+(i)} x_{ij}^k = 1 \quad \forall i \in T \tag{6}$$

$$\sum_{k \in K} \sum_{(f,j) \in \delta^+(f)} x_{fj}^k \le 1 \quad \forall f \in F \tag{7}$$

$$\sum_{(i,j) \in \delta^+(i)} x_{ij}^k - \sum_{(j,i) \in \delta^-(i)} x_{ji}^k = 0 \quad \forall i \in T \cup F, \forall k \in K \tag{8}$$

$$\sum_{r \in R} x_{fr}^k - \sum_{(i,f) \in \delta^-(f)} x_{if}^k = 0 \quad \forall f \in F, \forall k \in K \tag{9}$$

$$\sum_{(o,j) \in \delta^+(o)} x_{oj}^k - \sum_{(i,d) \in \delta^-(d)} x_{id}^k = 0 \quad \forall k \in K \tag{10}$$

$$s_i + t_i + t_{ij} - M(1 - \sum_{k \in K} x_{ij}^k) \le s_j \quad \forall i \in T, \forall (i,j) \in \delta^+(i) \tag{11}$$

$$s_f + U \cdot \delta + t_{fj} - M(1 - \sum_{k \in K} x_{fj}^k) \le s_j \quad \forall f \in F, \forall j \in T \tag{12}$$

$$s_f = \sum_{k \in K} \sum_{r \in R} s_r x_{fr}^k \quad \forall f \in F \tag{13}$$

$$y_i^k - e_i^k - e_{ij}^k + M(1 - \sum_{k \in K} x_{ij}^k) \geq y_j^k \quad \forall i \in T \cup \{o\}, \forall (i,j) \in \delta^+(i), \forall k \in K \tag{14}$$

$$\overline{y_f^k} - e_{fj}^k + M(1 - \sum_{k \in K} x_{fj}^k) \geq y_j^k \quad \forall f \in F, \forall j \in T, \forall k \in K \tag{15}$$

$$\sigma \cdot E^k \leq y_i^k \leq E^k \quad \forall i \in T \cup F, \forall k \in K \tag{16}$$

$$y_o^k = E^k \quad \forall k \in K \tag{17}$$

$$\overline{\tau_f^k} - \tau_f^k = U \cdot \delta \cdot \sum_{(f,j) \in \delta^+(f)} x_{fj}^k \quad \forall f \in F, \forall k \in K \tag{18}$$

$$y_f^k = \sum_{b \in B^k} \lambda_{fb}^k y_b^k \quad \forall f \in F, \forall k \in K \tag{19}$$

$$\tau_f^k = \sum_{b \in B^k} \lambda_{fb}^k t_b^k \quad \forall f \in F, \forall k \in K \tag{20}$$

$$\sum_{b \in B^k} \lambda_{fb}^k = \sum_{b \in B^k \setminus \{0\}} w_{fb}^k \quad \forall f \in F, \forall k \in K \tag{21}$$

$$\sum_{b \in B^k \setminus \{0\}} w_{fb}^k = \sum_{(f,j) \in \delta^+(f)} x_{fj}^k \quad \forall f \in F, \forall k \in K \tag{22}$$

$$\lambda_{f0}^k \leq w_{f1}^k \quad \forall f \in F, \forall k \in K \tag{23}$$

$$\lambda_{fb}^k \leq w_{fb}^k + w_{fb+1}^k \quad \forall f \in F, \forall k \in K, \forall b \in B^k \setminus \{0, m^k\} \tag{24}$$

$$\lambda_{fm^k}^k \leq w_{fm^k}^k \quad \forall f \in F, \forall k \in K \tag{25}$$

$$\overline{y_f^k} = \sum_{b \in B^k} \overline{\lambda_{fb}^k} y_b^k \quad \forall f \in F, \forall k \in K \tag{26}$$

$$\overline{\tau_f^k} = \sum_{b \in B^k} \overline{\lambda_{fb}^k} t_b^k \quad \forall f \in F, \forall k \in K \tag{27}$$

$$\sum_{b \in B^k} \overline{\lambda_{fb}^k} = \sum_{b \in B^k \setminus \{0\}} \overline{w_{fb}^k} \quad \forall f \in F, \forall k \in K \tag{28}$$

$$\sum_{b \in B^k \setminus \{0\}} \overline{w_{fb}^k} = \sum_{(f,j) \in \delta^+(f)} x_{fj}^k \quad \forall f \in F, \forall k \in K \tag{29}$$

$$\overline{\lambda_{f0}^k} \leq \overline{w_{f1}^k} \quad \forall f \in F, \forall k \in K \tag{30}$$

$$\overline{\lambda_{fb}^k} \leq \overline{w_{fb}^k} + \overline{w_{fb+1}^k} \quad \forall f \in F, \forall k \in K, \forall b \in B^k \setminus \{0, m^k\} \tag{31}$$

$$\overline{\lambda_{fm^k}^k} \leq \overline{w_{fm^k}^k} \quad \forall f \in F, \forall k \in K \tag{32}$$

$$\sum_{f \in F} x_{fr}^k + \sum_{u=1, \overline{r}=b^u(r)}^{U-1} \sum_{f \in F} x_{f\overline{r}}^k \leq C_r \quad \forall r \in R, \forall k \in K \tag{33}$$

$$x_{ij}^k \in \{0,1\} \quad \forall (i,j) \in A \cup I, \forall k \in K \tag{34}$$

$$w_{fb}^k, \overline{w_{fb}^k} \in \{0,1\} \quad \forall f \in F, \forall b \in B^k, \forall k \in K \tag{35}$$

$$\lambda_{fb}^k, \overline{\lambda_{fb}^k} \geq 0 \quad \forall f \in F, \forall b \in B^k, \forall k \in K \tag{36}$$

The objective is to minimize the total operating cost, including the vehicle depreciation cost z_1, the electricity cost z_2 and the labor cost z_3. The vehicle cost equals the sum of daily depreciation cost of the bus fleet, where c^k is the daily depreciation cost of a single bus of type k. The electricity cost includes the expenses of partial recharging during operation and fully recharging after finishing all tasks. The labor cost in this paper is similar to the time-dependent service costs unrelated to energy consumption defined in Rogge et al. (2018), where c_t represents the labor cost per minute for service trips and deadhead trips.

Constraint (6) ensures that every service trip is fulfilled exactly once. Constraint (7) ensures that every possible recharging event can be performed at most once. Constraint (8) requires flow conservation. Constraint (9) ensures that all performed recharging

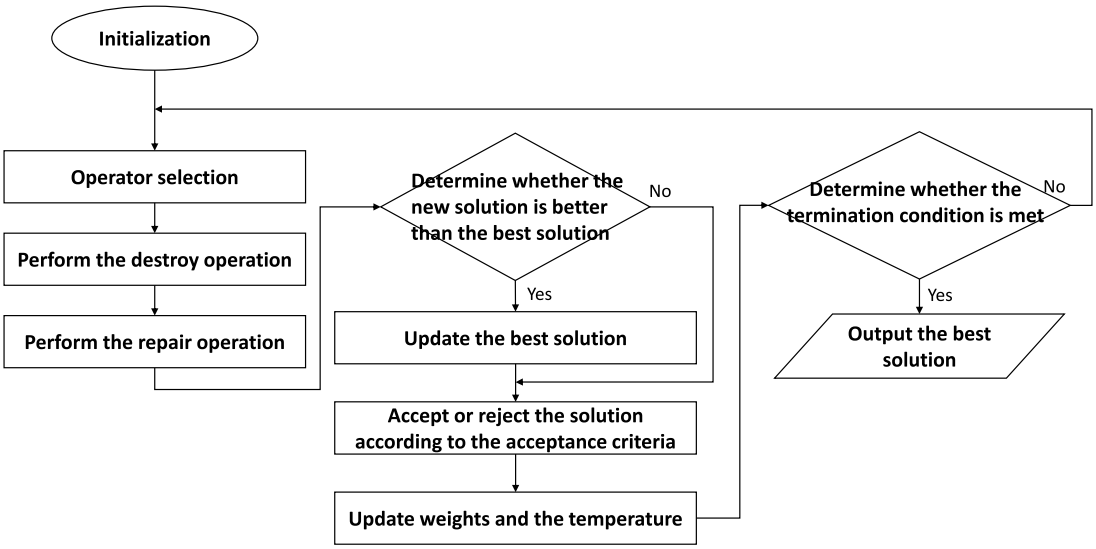

Fig. 5. Flow chart of the algorithm.

events are assigned to a recharging time division. Constraint (10) enforces that the number of buses that are departed from and returned to the depot is the same. Constraints (11) to (12) specify the time compatibility of the connection between service trip and recharging event nodes and their subsequent nodes, respectively, where M is a sufficiently large positive number. Constraint (13) enforces that the start time of the recharging event node is consistent with the start time of the time division it links to. Constraints (14) and (15) ensure the energy consumption compatibility of the connection between nodes. Constraint (16) and (17) specify the range of remaining battery power. Constraint (18) ensures the corresponding charging duration in the piecewise linear charging function is equal to $U \cdot \delta$. Constraint (19) to (25) define the battery power and corresponding charging time according to the charging function when a recharging event starts. Similarly, constraint (26) to (32) define the battery power and corresponding charging time at the end of a recharging event. Constraint (33) is the charging station capacity constraint. A detailed illustration of the piecewise linear charging function and charging station capacity constraints are shown in Appendix B. The domain of variables is defined by constraint (34) to (36).

3.4. Optimization algorithm

The ALNS algorithm (Ropke and Pisinger, 2006), which is widely used for varied kinds of EVSP with high efficiency (Wen et al., 2016; Zhang et al., 2021a), is employed to solve the EVSP-CSC-NL in this paper. The ALNS explores the neighborhood by destroying and repairing the current solution to increase the search range of the search space, and improve the probability of obtaining a better solution. Fig. 5 illustrates the flow chart of the algorithm. A greedy insertion algorithm (Adler and Mirchandani, 2017) is used to construct initial solutions. A roulette wheel selection and an adaptive weight adjustment method (Ropke and Pisinger, 2006) are employed for operator selection, and the simulated annealing algorithm is used as the acceptance criteria. The algorithm terminates when n iterations are executed, or n' iterations occur without improvements. All hyper-parameters of the ALNS are tuned before generating the solution.

3.4.1. Destroy operators

In each iteration, θ trips and their recharging nodes are removed from the solution by a destroy operator with certain rules, where θ is a random integer between $[\theta_{min}, \theta_{max}]$. Trip chains with fewer than two trips are removed to minimize the number of vehicles.

Three types of operators are used in this study, including a random removal, a time-related removal, and a neighbor-based removal. In the time-related removal, the temporal relationship $R(i,j)$ between trip i and j is redefined as $w_1 \cdot \mid s_i - s_j \mid + w_2 \cdot \mid t_i - t_j \mid$, where s_i and s_j are the start time of trip i and j, and t_i and t_j are the travel time of trip i and j. w_1 and w_2 denote the weights of the two values, respectively. A smaller $R(i,j)$ indicates that the time correlation between two trips is greater. When performing the time-related removal, one trip is first removed randomly, then one of the removed trips is randomly selected, and the trip with the strongest temporal relationship is removed, and the process is repeated until θ trips are removed. The neighbor-based removal removes one trip with the trips before and after in the current trip chain each time, expanding the range of single removals, and giving more insertion space for other trips.

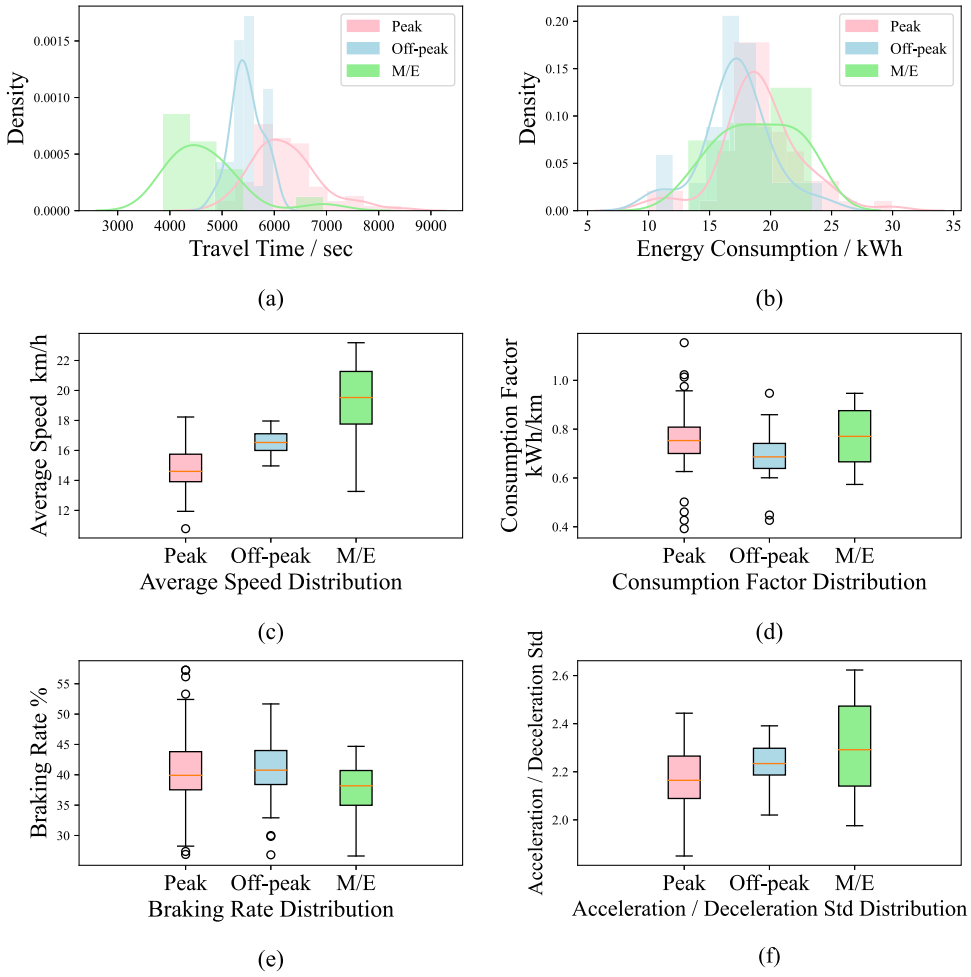

Fig. 6. KDE plot and distribution of operation data in different periods *(M/E refers to the morning/evening period)*.

3.4.2. Repair operators

For EVSP-CSC-NL, the repair of the solution includes the insertion of the service trip and recharging event nodes, and the selection of the vehicle type. In this paper, two repair operators, namely random insertion and greedy insertion, are used.

The random insertion aims to ensure the diversity of solutions and prevent local optimum. In each iteration, one removed trip is randomly selected and inserted into a random position that is compatible with the preceding and the following trip. If no position is compatible, the trip would be inserted into a new trip chain with a randomly assigned vehicle type. After each inserted trip, the recharging node is inserted with a probability p_{charge} and randomly assigned to a time-compatible recharging time division. Note that the night charging scenario can be realized by setting $p_{charge} = 0$ in the optimization algorithm.

The greedy insertion operator is used to generate feasible solutions as much as possible to ensure the convergence of the algorithm. The insertion cost equals the added deadhead trip distance after insertion (Wen et al., 2016; Zhang et al., 2021a). In a single depot scenario, however, the distance of deadhead trips among different trips is the same. To reduce the computation time, the greedy insertion uses the same node insertion method as the random insertion, and selects the compatible and available recharging time division for each recharging node. When all nodes are inserted, the greedy insertion is applied again to replace BEBs with lower-cost alternatives while keeping the trip chain unchanged. The replacement is accepted if the total cost decreases and all constraints are met.

3.4.3. Penalty

This paper defines penalties for solutions that violate constraints. Specifically, the algorithm checks whether the generated solution violates the energy compatibility constraints and charging station capacity constraints, and adds the energy penalty $c^{ene}_{penalty}$ and the charging station capacity penalty $c^{cap}_{penalty}$ to the total cost accordingly. The algorithm determines whether to accept an infeasible solution by the acceptance criteria defined by the simulated annealing. Finally, the optimal solution is required to be feasible.

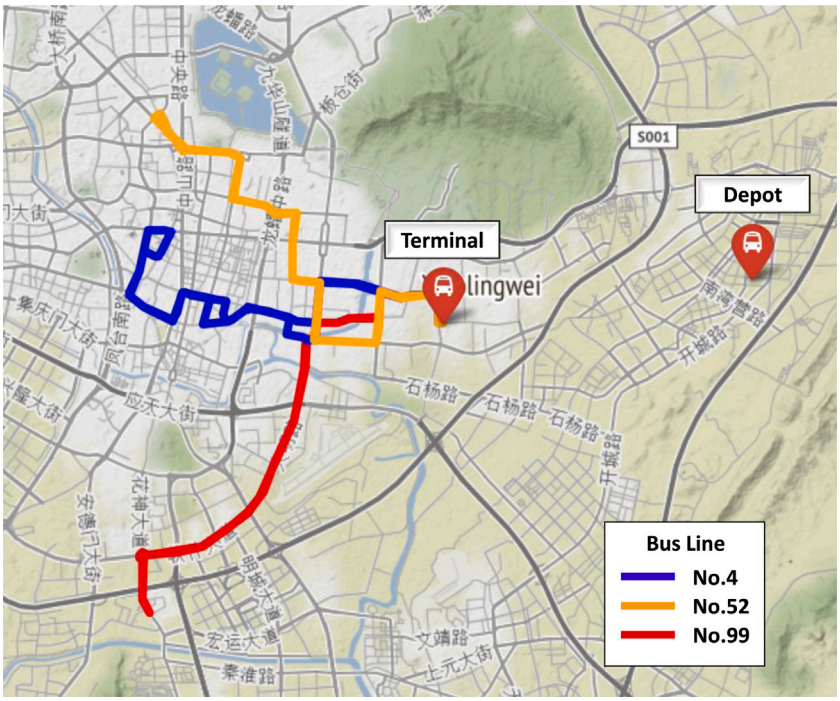

Fig. 7. The bus network with three bus lines.

4. Results and discussions

4.1. Energy consumption distribution of BEB

Based on the clustered dataset of Line 4, the travel time, energy consumption, average speed, energy consumption factor, braking rate and standard deviation of acceleration/deceleration for each period are calculated, and the results are shown in Fig. 6. The consumption factor is the energy consumption per unit distance traveled by the vehicle (kWh/km). The braking rate equals the accumulated time that the driver presses the brake pedal divided by the total travel time in a single trip, and is used to describe the frequency of braking behavior.

Fig. 6(a) and (b) present the kernel density estimation (KDE) plots of travel time and energy consumption for three periods. The trip travel time in the peak period is the highest with an average travel time of 103 min, followed by the off-peak period, while the travel time is significantly shorter during the morning/evening period. The energy consumption during the peak period is generally higher than those in the off-peak period. The distribution of trip energy consumption during the morning/evening period is more dispersed, indicating a higher uncertainty of driving operations.

To further summarize the characteristics of each period, the boxplots of four trip features are plotted in Fig. 6(c) to (f). Trips in the peak period exhibit relatively low average speed and high energy consumption, probably due to the congested road conditions during peak hours. In contrast, higher average speeds of BEBs during the off-peak period lead to lower energy consumption factors than during the peak period. However, the average energy consumption factor for trips during the morning/evening period is high despite their high speed. This is due to more aggressive driving behavior presented as high average speed, low braking rate and frequent acceleration.

4.2. Case study

4.2.1. Parameter values

In the case study, the single-line network (Line 4) is expanded to a real-world multi-line network (Line 4, 52 and 99), which shares the same depot and terminal in Nanjing, China. The roundtrip mileage of each route is 24.8 km, 25.8 km and 25.4 km, respectively. The network contains a total of 275 service round trips per day, each containing a pair of consecutive dispatching and returning trips. As shown in Fig. 7, the terminal has 20 chargers with 60 kW power output each, providing parking and recharging services for BEBs. The depot where BEBs park and get charged at night is 10 kilometers away from the terminal. Trip travel time and energy consumption of Line 52 and Line 99 are scaled based on that of Line 4. With similar road geometry, traffic conditions and distance of the three lines as well as the uncertainty introduced by Monte Carlo simulation in the sample generation process, the difference in the energy consumption distribution among bus lines is negligible. However, note that the size of the empirical

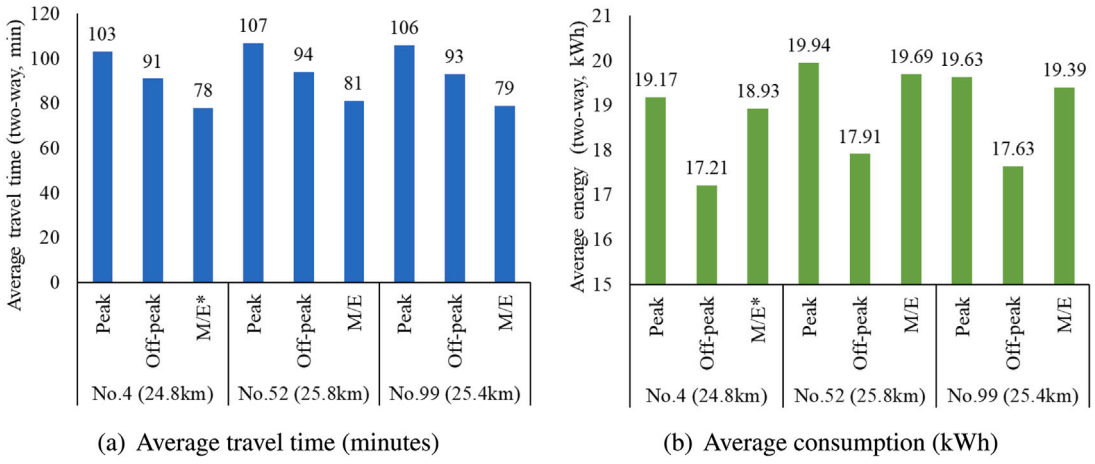

Fig. 8. Average trip data of three bus lines *(two-way, M/E refers to the morning/evening period)*.

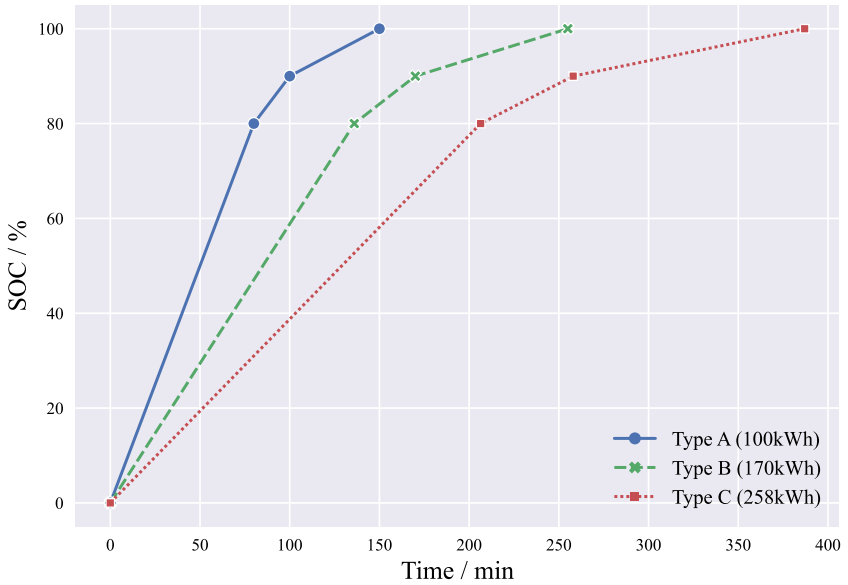

Fig. 9. Piecewise linear approximation for different vehicle types.

Table 2
BEB type information.

Vehicle type	A	B	C
Battery capacity (kWh)	100	170	256
Daily depreciation (CNY/day)	804.70	907.56	1039.14

dataset is one of the limitations of this study. For larger networks with multiple bus line types, more vehicle operation data should be obtained to estimate trip energy consumption. Fig. 8 shows the average travel time (a) and trip energy consumption (b). A hundred service trip samples consisting of three bus lines in one day are generated using the method in Section 3.2.

To investigate the impact of different vehicle types, this study considers three BEB types varied by the capacity and the cost shown in Table 2, according to the data of Skywell NJL6100EV(H10) series (Skywell, 2022). The daily depreciation cost is calculated assuming an average lifetime of 7.8 years per BEB and 360 days of operation annually (Wang et al., 2017). Considering the influence of battery size on energy consumption, an energy consumption growth coefficient generated from the result of Ji et al. (2022) is used to adjust the energy consumption of different vehicle types. The detailed steps are introduced in Appendix C. The electricity price c_e for BEB charging in Nanjing is 0.6416 CNY/kWh. The average salary of a bus driver is 5,500 CNY per month, or 0.5 CNY/minute (averaged by 22 working days per month and 8 h per day). The lowest allowable SOC σ to use the bus is 20%.

Table 3
Parameters of breakpoints defined in Section 3.3.2.

Index (b)	SOC/%	Charging time (t_b^k)/min		
		k = A	k = B	k = C
0	0	0	0	0
1	80	80	136	206
2	90	100	170	258
3	100	150	255	387

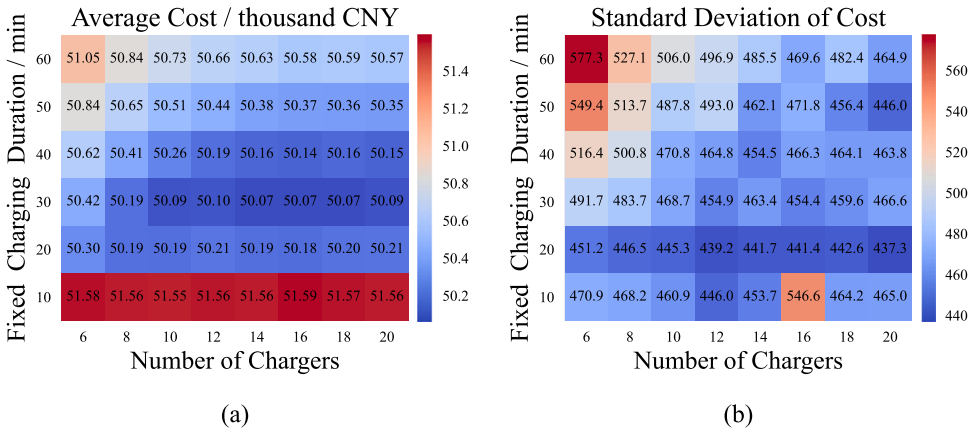

Fig. 10. Heat map of the mean and standard deviation of operation cost in different scenarios (blue represents lower values; red represents higher values). (For interpretation of the references to color in this figure legend, the reader is referred to the web version of this article.)

The piecewise nonlinear charging function of three bus types is illustrated in Fig. 9. Batteries get charged at the maximum charging rate when the SOC is lower than 80%; then the slope of the charging curve becomes smoother with lower charging power (Hõimoja et al., 2012). Table 3 shows the parameters of breakpoints that are used in Section 3.3.2.

4.3. Optimization result analysis

This section compares the optimal cost with varied charging strategies, charging durations, and the number of chargers. The charging duration is set in the range of 10 to 60 min with the interval of 10 min, and the number of chargers is set in the range of 6 to 20 with the interval of 2. In total, 48 scenarios with different sets of parameter combinations are tested. One hundred samples, each representing a daily service trip set, are generated as the input of the optimization program using the method proposed in Section 3.2. Each set of parameter combinations is applied to these samples to simulate the uncertain travel time and energy consumption. The result robustness is demonstrated by the standard deviation of random samples.

4.3.1. Cost-effectiveness and robustness

Fig. 10 presents the mean and standard deviation of the optimized operation cost from 100 samples per scenario. The average cost reflects the average performance of each parameter combination and the standard deviation represents the adaptability of each parameter combination to uncertain travel time and energy consumption.

When the fixed charging duration is 10 min, the average cost is significantly higher than the others, and it decreases by 2.63% when the fixed charging duration changes to 20 min. When the fixed charging duration exceeds 40 min, the total cost and the standard deviation tend to rise. The scenario comparison shows that a fixed charging duration of 30 to 40 min has a lower operation cost and stronger robustness of the optimization results, which can be demonstrated by the standard deviation.

When the same fixed charging duration is employed, the average cost decreases with an increasing charging station capacity; then the average cost keeps stable when the number of chargers reaches a certain threshold. At the same time, the standard deviation tends to drop as the number of chargers increases, indicating an improved resilience to uncertain environments. In addition, average costs under different fixed charging durations exhibit different sensitivity to charging station capacity. For example, eight chargers in a station can serve the whole fleet when the fixed charging duration is 20 min, while the number increases to 16 if the fixed charging duration is 60 min. The result shows that bus operators can reduce the charging infrastructure assignment and maximize resource utilization through an optimized charging schedule while ensuring high economic efficiency and robustness. Under current resource conditions (20 chargers at one station), the most economical charging duration is 30 min, with 14 chargers in operation for the studied bus network. The average cost of the optimal scenario is around 50,065 CNY. The rest of chargers can open to public for additional profits, as has been practiced in Qingdao, China (Xinhua, 2022).

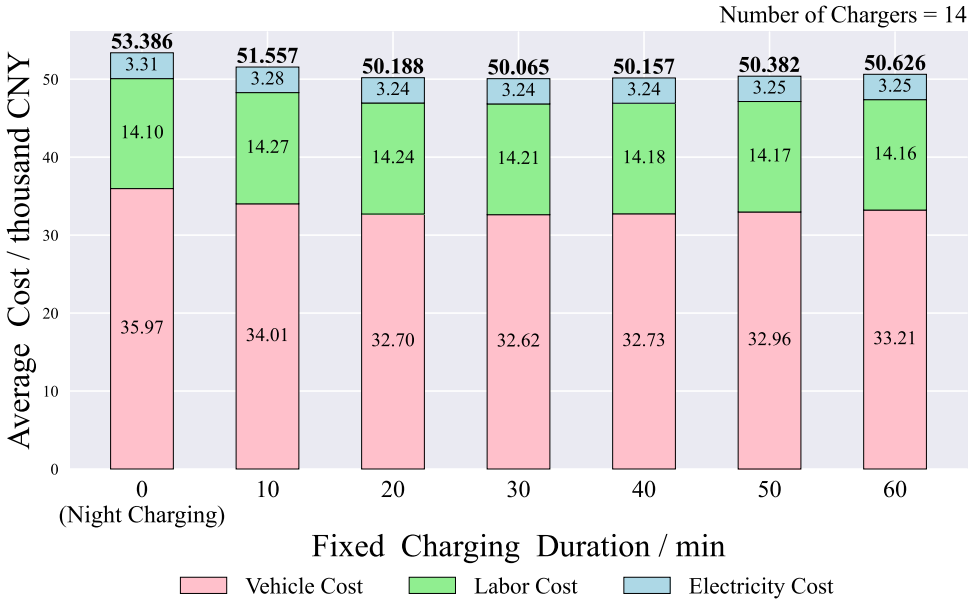

Fig. 11. Impact of fixed charging duration on operation cost (number of chargers = 14).

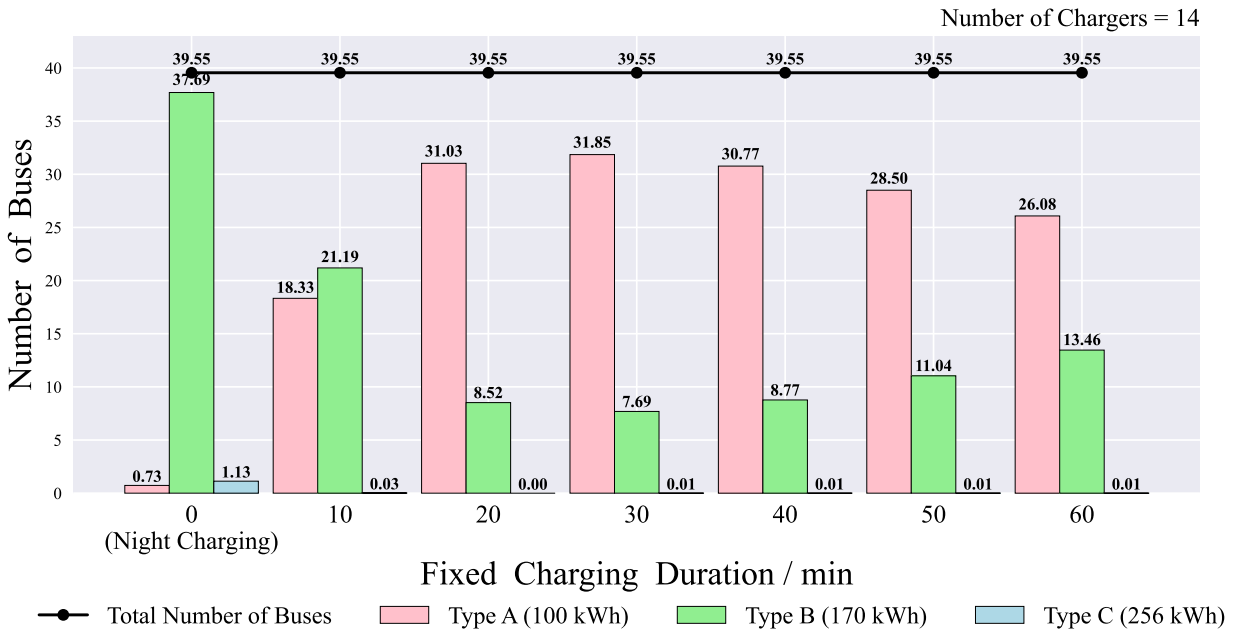

Fig. 12. Average number of buses required when different fixed charging durations are adopted (number of chargers = 14).

4.3.2. Impact of the fixed charging duration

Fig. 11 shows the average cost and the cost composition under different fixed charging duration when the number of chargers is 14 (the optimal scenario based on Section 4.3.1). The operation cost is mainly composed of vehicle depreciation costs and labor costs. The electricity cost accounts for a smaller proportion, with an average of 6.40%. A negative correlation between the labor cost and the charging duration can be observed since an increasing charging duration leads to a decreasing number of recharging events, thus reducing the distance of deadhead trips and working hours.

The night charging strategy, in which the vehicles are not allowed to be charged during the daytime and is widely used in practice, is used as the benchmark to illustrate the cost-effectiveness of the optimized charging plan. The average cost of night

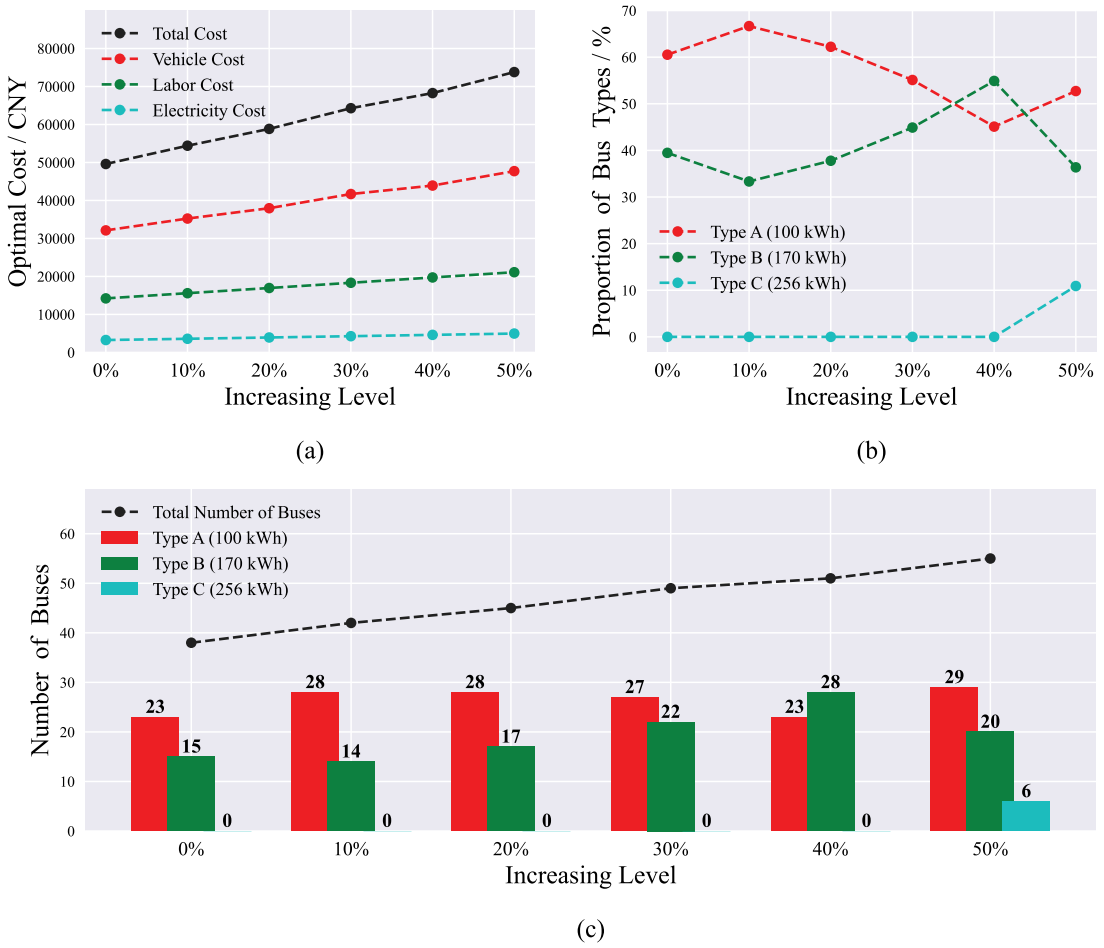

Fig. 13. Optimal cost (a), the proportion of bus types (b), and fleet composition (c) when the average travel time and energy consumption are increased by different levels.

charging is higher than the optimized charging plan by 6.63%, reaching 53,386 CNY. When it exceeds 30 min, the average total cost slightly increases due to higher bus depreciation costs. Nevertheless, the average cost of a 60-minute fixed charging duration is still 5.17% lower than that of night charging.

The high cost of night charging can be explained by Fig. 12, which shows the average number of vehicles of three types. Although the variation in the total number of vehicles is minimal, different fleet composition can be observed by the proportion of different vehicle types. When night charging is performed, the fleet is mainly composed of type B (95.30%) and type C (2.86%) buses with higher battery capacity. When vehicles are allowed to be charged during the operation time, the number of type A grows significantly to 78.80%, especially when the fixed charging duration equals 30 min. Note that in this paper, the electricity price is constant, which is aligned with the current electricity supply in Nanjing.

Analyzing the relationship between the vehicle depreciation cost and the fleet composition, we found that when the duration is too short (such as 10 min), the SOC after recharging cannot support multiple consecutive trips. In this case, vehicles with higher capacity are required to keep the bus service, increasing the depreciation cost. On the other hand, if the duration is too long (such as 1 h), to maintain the service, the network needs more vehicles or substitutes lower-capacity buses with their higher-capacity counterparts, leading to higher depreciation costs as well. In contrast, when the charging duration is 30 to 40 min, the buses can retain sufficient SOC after each recharging event while meeting the service constraints; thus, buses with lower battery capacity can fit into the schedule. The comparison demonstrates that a more flexible while sufficient charging duration is needed in order to make full utilization of smaller buses with lower battery capacity.

4.4. Results for bus routes with longer distances

In order to test the sensitivity of the resource assignment to the bus energy consumption, five synthetic bus networks are constructed based on real-world data. In these five networks, we assume a longer route distance with similar energy consumption

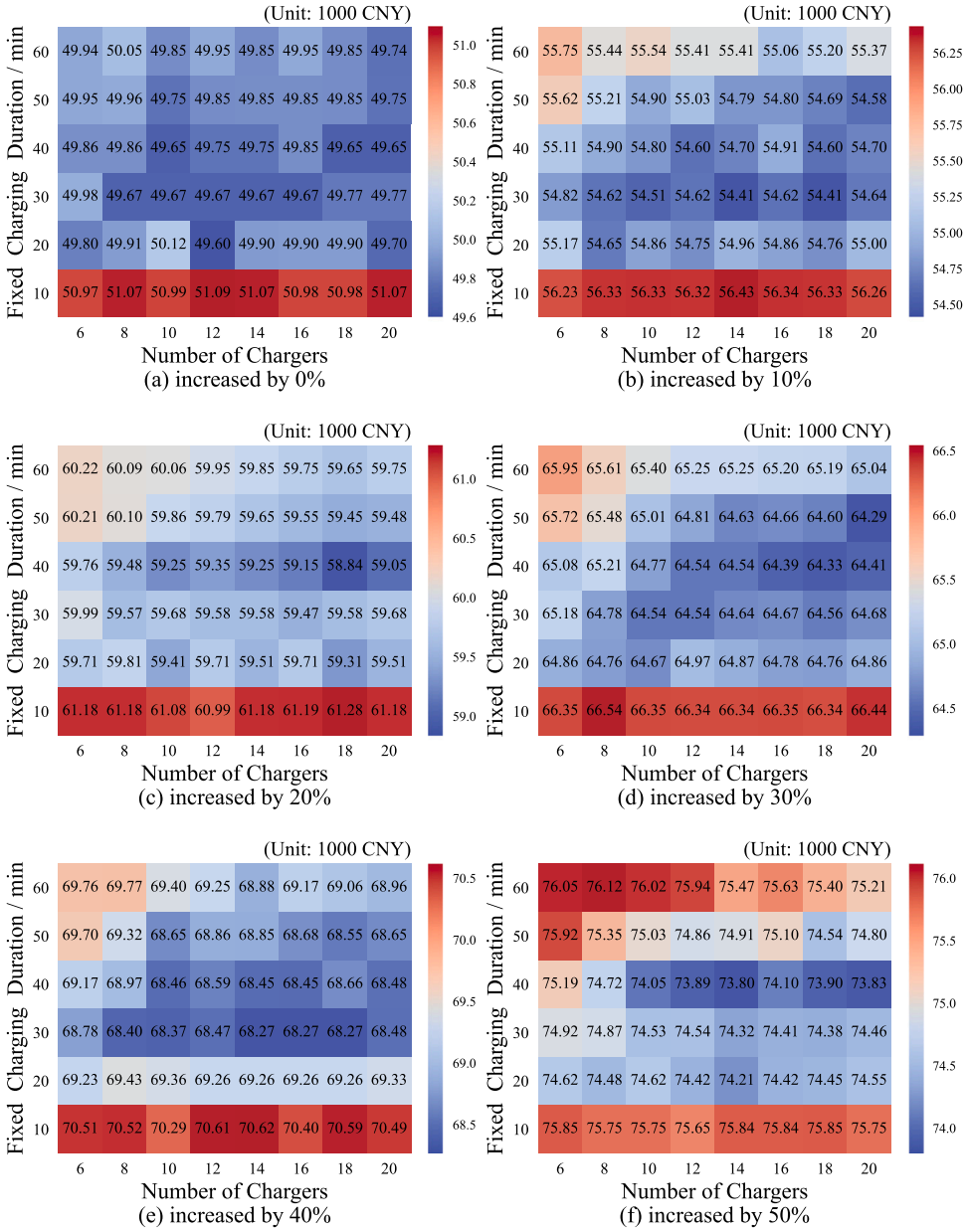

Fig. 14. Heat maps of operation costs under each fixed charging duration and charging station capacity when the average travel time and energy consumption are increased by different levels *(a to f indicates the increasing rate of 0% to 50% with the incremental of 10%)*.

rate and the same trip starting time. Accordingly, the average energy consumption and trip duration are scaled up by 10% (S1), 20% (S2), 30% (S3), 40% (S4), and 50% (S5), respectively, based on the aforementioned case (S0). The optimal results from 48 scenarios, which is the same as Section 4.3.1, are shown in Fig. 13.

The optimal total cost and sectional costs show a linear increase over the increasing energy level in Fig. 13(a). Compared to the base case where no scaling up is performed, the total cost increases to 73,798 CNY (48.79%) in S5, 64.47% of which comes from the vehicle depreciation. For every 10% increment, 3.4 more vehicles are required.

The proportion of bus types has a different trend from the total cost, as illustrated in Fig. 13(b). In S2 where the energy consumption and travel time are increased by 20%, the optimal fleet is still composed of type A (62.22%) and B (37.78%), which is similar to S0. As the energy consumption and travel time grow, the proportion of type A drops, reaching the lowest point of 45.10% at S4. At the same time, more vehicles of type B and type C are required.

When the trip energy consumption increases by 20% to 30% (S2 and S3), smaller buses can fulfill most of the service tasks with the optimal charging schedule. This scenario corresponds to an average of 31 km round trip, which can cover most urban

bus routes in metropolitan areas (The Ministry Of Transport, People's Republic of China, 2020). Even in S5 (38 km round trip on average), buses with small to medium battery sizes are still the most cost-effective options. In practice, however, most operators do not have confidence in small-capacity vehicle types, and are conservative in fleet composition, resulting in a waste of vehicle costs. We recommend allocating buses with a lager battery capacity to the lines with longer distances, such as suburban connection routes. In the urban scope, cheaper buses with smaller battery capacity can effectively reduce daily operation cost. The result also highlights the need to adopt the optimized charging plan, which leads to substantial savings from fleet composition.

The increase in energy consumption and travel time also has implications for the selection of fixed charging duration and resource assignment. As shown in Fig. 14, when the trip distance increases, the range of the optimal charging duration gradually converges to 30–40 min. Similarly, the cost-effective charging station capacity converges to the range of 14 to 20. A resource allocation strategy can be derived from the result. Generally, for single-depot bus services with 200–300 trips, the minimum charging station capacity of 14 can serve the optimal charging strategy with high robustness. The optimal recharging duration is varied from different energy consumption per trip, while the duration of 30–40 min can ensure sufficient SOC and stable services.

5. Conclusion

In this study, an electric vehicle scheduling problem considering charging station capacity and nonlinear charging (EVSP-CSC-NL) is proposed and formulated. An adaptive large neighborhood search (ALNS) algorithm is developed with novel destroy/repair operators to solve the optimization problem. Trip-based energy consumption and its uncertainties of BEBs are captured using global positioning system (GPS) trajectories and on-board diagnostics (OBD) data. In order to simulate possible uncertain conditions of BEB operation, energy consumption and travel time samples are generated from the average travel time-based trip clusters. Forty-eight scenarios are designed from six levels of charging duration and eight levels of charging station capacity.

The results show that recharging during the daytime operation can reduce costs by up to 6.63% compared to the night charging scenario. An increasing proportion of smaller-capacity buses due to the optimized daytime recharging is one of the major contributors to the reduced cost. Meanwhile, the fleet composition is significantly affected by the fixed charging duration. The ratio of vehicle types with the smallest capacity reaches 78.80% when the charging duration equals 30 min, leading to the lowest average cost of 50,065 CNY. Although sufficient charging resources can improve the robustness of the vehicle schedules, operators can reduce the investment in charging infrastructure if the energy demand of the bus network is moderate, because the marginal benefit decreases with more chargers at one station.

To examine the impact of energy consumption level on the optimal charging plan, energy consumption and duration time of each trip are increased by 10% to 50% with an interval of 10%. The result shows that buses with low-to-medium battery capacities can fulfill most of the service trips in metropolitan areas, even when the energy consumption level is increases by 50%, representing an extreme operation scenario in the city scale. For bus networks running in the single-depot mode with a similar trip size as our study, we recommend 30 to 40 min for each recharging event, and 14–20 slow-chargers (60 kW) can be sufficient to serve the network optimally. For existing infrastructure, the rest of the chargers in the terminal can open to public for additional profits.

The result of this study can be a reference of proper charging planning and resource assignment for urban electric bus systems. In future work, flexible charging duration should be considered to further reduce the operation cost, and algorithms with higher computational efficiency should be developed for larger-scale networks. The battery degradation process can also be integrated for a life-cycle assessment. In addition, the time-of-use (TOU) electricity pricing strategy has been implemented in many other cities to promote nighttime charging with lower fees, while the cooperative optimization considering the electricity grid and the bus operation needs to be further discussed.

CRediT authorship contribution statement

Qiuzi Chen: Conceptualization, Data processing, Algorithm development, Result analysis, Manuscript drafting and revision. **Chenming Niu:** Data processing. **Ran Tu:** Conceptualization, Manuscript revision, Supervision. **Tiezhu Li:** Data curation. **An Wang:** Manuscript revision. **Dengbo He:** Manuscript revision.

Acknowledgments

This study is funded by the National Natural Science Foundation of China for Young Scholars (No. 52102409), the Provincial Natural Science Foundation of Jiangsu Province for Young Scholars (No. BK20210246), National Natural Science Foundation of China (No. 42261144745), the Volkswagen-China Environmental Protection Foundation Automobile Innovation Plan, and the China Association for Science and Technology-Youth Talent Program. We thank Jian Sun from Skywell Automobile, Nanjing, for supporting the bus data.

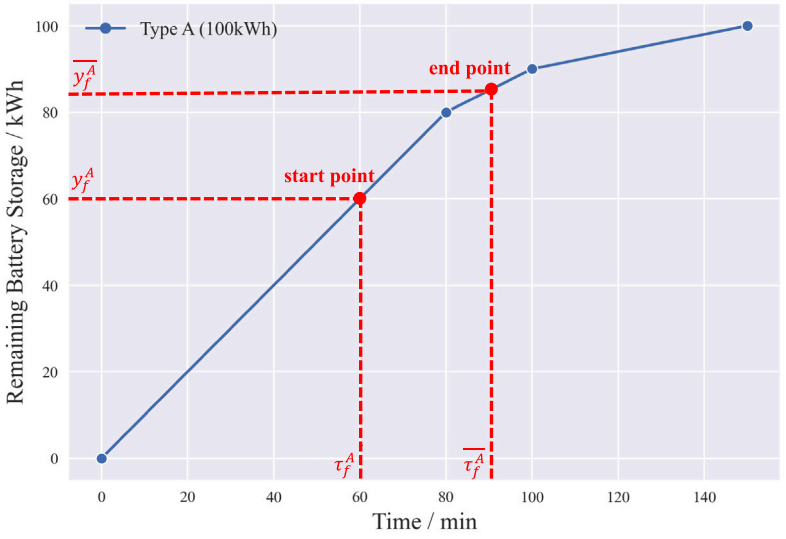

Parameters of breakpoints

b	0	1	2	3
t_b^A / min	0	80	100	150
y_b^A / kWh	0	80	90	100

Variables of the start point

b	0	1	2	3
w_{fb}^A / min	-	1	0	0
λ_{fb}^A / kWh	0.25	0.75	0	0
τ_f^A / min	60			
y_f^A / kWh	60			

Variables of the end point

b	0	1	2	3
$\overline{w_{fb}^A}$ / min	-	0	1	0
$\overline{\lambda_{fb}^A}$ / kWh	0	0.5	0.5	0
$\overline{\tau_f^A}$ / min	90			
$\overline{y_f^A}$ / kWh	85			

Fig. 15. Illustration of the piecewise linear charging function.

Appendix A

Sets:

K	Set of vehicle types indexed by k
D	Set of depots, $D = \{o, d\}$
T	Set of service trip nodes
F	Set of recharging event nodes indexed by f
N	Set of nodes, $N = D \cup T \cup F$
R	Set of recharging time division indexed by r
A	Set of arcs representing deadhead trips between nodes
I	Set of recharging time indicators
$\delta^-(i)$	Set of arcs that end at node $i \in N$
$\delta^+(i)$	Set of arcs that start at node $i \in N$
B^k	Set of breakpoints in the piecewise linear charging function for vehicle type $k \in K$

Parameters:

E^k	Battery capacity of vehicle type $k \in K$
σ	The safety level of battery state of charge
s_i	Start time of service trip $i \in T$
t_i	Travel time of service trip $i \in T$
e_i^k	Energy consumption of service trip $i \in T$ when performed by vehicles of type $k \in K$
t_{ij}	Travel time of deadhead trip $(i, j) \in A$
e_{ij}^k	Energy consumption of deadhead trip $(i, j) \in A$ when performed by vehicles of type $k \in K$
s_r	Start time of recharging time division $r \in R$
C_r	Charging station capacity at recharging time division $r \in R$
β	Fixed time interval
U	The number of unit intervals in one recharging event
$b^u(r)$	Time division u intervals ahead of $r \in R$
c^k	Depreciation cost of vehicle type $k \in K$
c_e	Unit charging cost
c_t	Unit labor cost

m^k	Number of breakpoints in the piecewise linear charging function for vehicle type $k \in K$
t_b^k	Charging time corresponding to breakpoint $b \in B^k$ for vehicle type $k \in K$
y_b^k	Battery power corresponding to breakpoint $b \in B^k$ for vehicle type $k \in K$
Decision variables:	
x_{ij}^k	Binary variable, taking a value of 1 if deadhead trip arc $(i, j) \in A$ is linked with a vehicle of type $k \in K$ and 0 otherwise
x_{fr}^k	Binary variable, taking a value of 1 if recharging event $f \in F$ begins at time division $r \in R$ with a vehicle of type $k \in K$ and 0 otherwise
Auxiliary variables:	
y_i^k	Remaining battery power of a vehicle of type $k \in K$ at the beginning of node $i \in N$
$\overline{y_f^k}$	Remaining battery power of bus of type $k \in K$ when recharging event $f \in F$ is finished
s_f	Start time of recharging event $f \in F$
τ_f^k	Corresponding start time in the charging function of recharging event $f \in F$ for vehicle type $k \in K$
$\overline{\tau_f^k}$	Corresponding end time in the charging function of recharging event $f \in F$ for vehicle type $k \in K$
w_{fb}^k	Binary variable, taking a value of 1 if the start battery power of recharging event $f \in F$ is between y_{b-1}^k and y_b^k for vehicle type $k \in K$, where $b \in B^k \setminus \{0\}$
$\overline{w_{fb}^k}$	Binary variable, taking a value of 1 if the end battery power of recharging event $f \in F$ is between y_{b-1}^k and y_b^k for vehicle type $k \in K$, where $b \in B^k \setminus \{0\}$
λ_{fb}^k	Coefficient associated with the breakpoint $b \in B^k$ in the piecewise linear charging function of vehicle type $k \in K$ at the beginning of the recharging event $f \in F$
$\overline{\lambda_{fb}^k}$	Coefficient associated with the breakpoint $b \in B^k$ in the piecewise linear charging function of vehicle type $k \in K$ at the end of the recharging event $f \in F$

Appendix B

In this study, the piecewise linear formulation of the charging function (Zhang et al., 2021a) is adopted. Fig. 15 shows how values of start and end points in a charging process are determined by auxiliary variables. As the remaining battery storage of the start point $y_f^A = 60$ kWh, the start time τ_f^A and other variables are determined according to Constraint (19) to (25). Constraint (22) enforces that only one of w_{fb}^A equals 1. Constraint (23) to (25) ensure that only two of λ_{fb}^A related to adjacent breakpoints are non-zero, and add up to 1 according to Constraint (21). Therefore, Constraint (19) makes y_f^A a linear combination of the parameters of two adjacent breakpoints, the solution of which is unique, and thus the values of λ_{fb}^A and τ_f^A can be determined. By assuming fixed charging durations, the end time of the charging process $\overline{\tau_f^A}$ are calculated by Constraint (18), and values of other variables of the end point can be determined similarly by Constraint (26) to (32).

Constraint (33) is the charging station capacity constraint ensuring that the number of vehicles being recharged or starting charging cannot exceed the capacity of the charging station at any time division $r \in R$. By predefining the time interval and charging duration, the total number of buses at a certain time can be converted to the sum of arcs that are linked to certain time-expanded nodes. As shown in Fig. 16, when the time interval and charging duration are equal to 10 min and 30 min, respectively, the number of buses in the charging station at 8:30 can be calculated as the sum of arcs linked to time-expanded node b (8:10–8:40), c (8:20–8:50) and d (8:30–9:00).

Appendix C

Ji et al. (2022) develop a regression model to estimate the trip energy consumption of BEBs, which shows a high estimation accuracy on empirical data. According to the sensitivity analysis, the energy consumption rate of BEB shows an approximately positive linear relationship with battery capacity. An energy consumption growth coefficient $\alpha = 2.97 \times 10^{-4}$ kWh/km kWh^{-1} is obtained from the aforementioned results, indicating that for every 1 kWh increase in battery capacity, energy consumption rate increases by 2.97×10^{-4} kWh/km. To adjust the energy consumption of different vehicle types, the energy consumption of trip $i \in T$ with vehicle type $k \in K$ is calculated by Eq. (37), where $\hat{E}$ is the benchmark capacity of BEBs whose GPS and OBD data was collected, $\hat{e}_i$ is the energy consumption of trip i obtained from collected data, and l_i is the travel distance of trip i.

$$e_i^k = \hat{e}_i + (E^k - \hat{E}) \cdot \alpha \cdot l_i \tag{37}$$

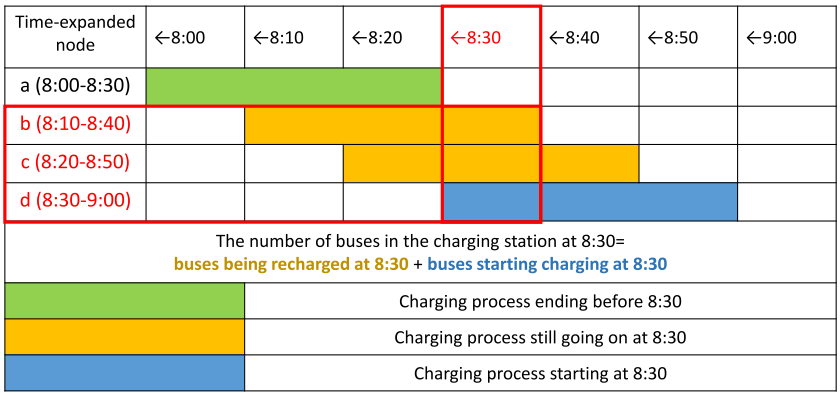

Fig. 16. Illustration of the time-expanded nodes *(Time interval=10 min, charging duration=30 min)*.

References

Adler, Jonathan D., 2014. Routing and scheduling of electric and alternative-fuel vehicles. Tech. rept., Arizona State University.

Adler, Jonathan D., Mirchandani, Pitu B., 2017. The vehicle scheduling problem for fleets with alternative-fuel vehicles. Transp. Sci. 51 (2), 441–456.

AMAP, 2022. AMAP API. Website. https://lbs.amap.com/api/webservice/guide/api/direction/.

Bie, Yiming, Ji, Jinhua, Wang, Xiangyu, Qu, Xiaobo, 2021. Optimization of electric bus scheduling considering stochastic volatilities in trip travel time and energy consumption. Comput.-Aided Civ. Infrastruct. Eng. 36 (12), 1530–1548.

Bunte, Stefan, Kliewer, Natalia, 2009. An overview on vehicle scheduling models. Public Transp. 1 (4), 299–317.

Dunn, J.B., Gaines, L., Kelly, J.C., James, C., Gallagher, K.G., 2015. The significance of Li-ion batteries in electric vehicle life-cycle energy and emissions and recycling's role in its reduction. Energy Environ. Sci. 8 (1), 158–168.

Farzaneh, Mohamadreza, Zietsman, Josias, Lee, Doh-Won, Johnson, Jeremy, Wood, Nicholas, Ramani, Tara, Gu, Chaoyi, et al., 2014. Texas-specific drive cycles and idle emissions rates for using with epa's MOVES model. Tech. rept., Texas. Dept. of Transportation. Research and Technology Implementation Office.

Gao, Yajing, Guo, Shixiao, Ren, Jiafeng, Zhao, Zheng, Ehsan, Ali, Zheng, Yanan, 2018. An electric bus power consumption model and optimization of charging scheduling concerning multi-external factors. Energies 11 (8), 2060.

He, Yi, Liu, Zhaocai, Song, Ziqi, 2020. Optimal charging scheduling and management for a fast-charging battery electric bus system. Transp. Res. Part E: Logist. Transp. Rev. 142, 102056.

He, Yi, Liu, Zhaocai, Song, Ziqi, 2022. Integrated charging infrastructure planning and charging scheduling for battery electric bus systems. Transp. Res. D 111, 103437, URL https://www.sciencedirect.com/science/article/pii/S1361920922002632.

Hõimoja, Hardi, Rufer, Alfred, Dziechciaruk, Grzegorz, Vezzini, Andrea, 2012. An ultrafast EV charging station demonstrator. In: International Symposium on Power Electronics Power Electronics, Electrical Drives, Automation and Motion. IEEE, pp. 1390–1395.

Jefferies, Dominic, Göhlich, Dietmar, 2020. A comprehensive TCO evaluation method for electric bus systems based on discrete-event simulation including bus scheduling and charging infrastructure optimisation. World Electr. Veh. J. 11 (3), URL https://www.mdpi.com/2032-6653/11/3/56.

Ji, Jinhua, Bie, Yiming, Zeng, Ziling, Wang, Linhong, 2022. Trip energy consumption estimation for electric buses. Commun. Transp. Res. 2, 100069, URL https://www.sciencedirect.com/science/article/pii/S2772424722000191.

Jiang, Mengyan, Zhang, Yi, 2021. Optimal electric bus scheduling under travel time uncertainty: A robust model and solution method. J. Adv. Transp. 2021.

Lajunen, Antti, Lipman, Timothy, 2016. Lifecycle cost assessment and carbon dioxide emissions of diesel, natural gas, hybrid electric, fuel cell hybrid and electric transit buses. Energy 106, 329–342.

Lee, Jinwoo, Shon, Heeseung, Papakonstantinou, Ilia, Son, Sanghoon, 2021. Optimal fleet, battery, and charging infrastructure planning for reliable electric bus operations. Transp. Res. D 100, 103066.

Li, Jing-Quan, 2014. Transit bus scheduling with limited energy. Transp. Sci. 48 (4), 521–539.

Liu, Kai, Gao, Hong, Liang, Zhe, Zhao, Meng, Li, Cheng, 2021. Optimal charging strategy for large-scale electric buses considering resource constraints. Transp. Res. D 99, 103009, URL https://www.sciencedirect.com/science/article/pii/S1361920921003072.

Montoya, Alejandro, Guéret, Christelle, Mendoza, Jorge E., Villegas, Juan G., 2017. The electric vehicle routing problem with nonlinear charging function. Transp. Res. B 103, 87–110, URL https://www.sciencedirect.com/science/article/pii/S0191261516304556. Green Urban Transportation.

Olsen, Nils, Kliewer, Natalia, Wolbeck, Lena, 2020. A study on flow decomposition methods for scheduling of electric buses in public transport based on aggregated time–space network models. CEJOR Cent. Eur. J. Oper. Res. 1–37.

Pelletier, Samuel, Jabali, Ola, Laporte, Gilbert, Veneroni, Marco, 2017. Battery degradation and behaviour for electric vehicles: Review and numerical analyses of several models. Transp. Res. B 103, 158–187, URL https://www.sciencedirect.com/science/article/pii/S0191261516303794. Green Urban Transportation.

Perumal, Shyam S.G., Lusby, Richard M., Larsen, Jesper, 2021. Electric bus planning & scheduling: A review of related problems and methodologies. European J. Oper. Res..

Quarles, Neil, Kockelman, Kara M., Mohamed, Moataz, 2020. Costs and benefits of electrifying and automating bus transit fleets. Sustainability 12 (10), 3977.

Rinaldi, Marco, Picarelli, Erika, D'Ariano, Andrea, Viti, Francesco, 2020. Mixed-fleet single-terminal bus scheduling problem: Modelling, solution scheme and potential applications. Omega 96, 102070.

Rogge, Matthias, Van der Hurk, Evelien, Larsen, Allan, Sauer, Dirk Uwe, 2018. Electric bus fleet size and mix problem with optimization of charging infrastructure. Appl. Energy 211, 282–295.

Ropke, Stefan, Pisinger, David, 2006. An adaptive large neighborhood search heuristic for the pickup and delivery problem with time windows. Transp. Sci. 40 (4), 455–472.

Skywell, 2022. Skywell Product Page. Website. https://www.skywellcorp.com/index.php/product/detail/5.html.

Tang, Xindi, Lin, Xi, He, Fang, 2019. Robust scheduling strategies of electric buses under stochastic traffic conditions. Transp. Res. C 105, 163–182.

The Ministry Of Transport, People's Republic of China, 2020. National Report on Urban Passenger Transportation Development (2019).

The State Council of People's Republic of China, 2021. Modern comprehensive transportation system for 14th five-year plan. Website. http://www.gov.cn/zhengce/content/2022-01/18/content_5669049.htm.

Wang, Yusheng, Huang, Yongxi, Xu, Jiuping, Barclay, Nicole, 2017. Optimal recharging scheduling for urban electric buses: A case study in Davis. Transp. Res. Part E: Logist. Transp. Rev. 100, 115–132.

Wang, Yongxing, Liao, Feixiong, Lu, Chaoru, 2022. Integrated optimization of charger deployment and fleet scheduling for battery electric buses. Transp. Res. D 109, 103382.

Wen, Min, Linde, Esben, Ropke, Stefan, Mirchandani, P, Larsen, Allan, 2016. An adaptive large neighborhood search heuristic for the electric vehicle scheduling problem. Comput. Oper. Res. 76, 73–83.

Wu, Weitiao, Lin, Yue, Liu, Ronghui, Jin, Wenzhou, 2022. The multi-depot electric vehicle scheduling problem with power grid characteristics. Transp. Res. B 155, 322–347.

Wu, Zhixin, Wang, Michael, Zheng, Jihu, Sun, Xin, Zhao, Mingnan, Wang, Xue, 2018. Life cycle greenhouse gas emission reduction potential of battery electric vehicle. J. Clean. Prod. 190, 462–470.

Xinhua, 2022. Qingdao opens electric bus charging stations to public. Website. https://english.www.gov.cn/news/photos/202205/13/content_WS627dff71c6d02e533532aa59.html.

Yao, Enjian, Liu, Tong, Lu, Tianwei, Yang, Yang, 2020. Optimization of electric vehicle scheduling with multiple vehicle types in public transport. Sustainable Cities Soc. 52, 101862.

Yıldırım, Şule, Yıldız, Barış, 2021. Electric bus fleet composition and scheduling. Transp. Res. C 129, 103197.

Zhang, Aijia, Li, Tiezhu, Tu, Ran, Dong, Changyin, Chen, Haibo, Gao, Jianbing, Liu, Ye, 2021a. The effect of nonlinear charging function and line change constraints on electric bus scheduling. Promet-Traffic Transp. 33 (4), 527–538.

Zhang, Le, Wang, Shuaian, Qu, Xiaobo, 2021b. Optimal electric bus fleet scheduling considering battery degradation and non-linear charging profile. Transp. Res. Part E: Logist. Transp. Rev. 154, 102445, URL https://www.sciencedirect.com/science/article/pii/S136655452100209X.

Zhou, Yu, Meng, Qiang, Ong, Ghim Ping, 2022a. Electric bus charging scheduling for a single public transport route considering nonlinear charging profile and battery degradation effect. Transp. Res. B 159, 49–75, URL https://www.sciencedirect.com/science/article/pii/S0191261522000443.

Zhou, Yu, Wang, Hua, Wang, Yun, Li, Rui, 2022b. Robust optimization for integrated planning of electric-bus charger deployment and charging scheduling. Transp. Res. D 110, 103410, URL https://www.sciencedirect.com/science/article/pii/S136192092200236X.